JOURNAL OF SOLID STATE CHEMISTRY **140,** 219–225 (1998)
ARTICLE NO. SC987879

Hydrothermal Synthesis and Crystal Structure of Barium Hewettite: $BaV_6O_{16} \cdot nH_2O$

Yoshio Oka,*[,1] Takeshi Yao,† Shoichi Sato,‡ and Naoichi Yamamoto§

*Department of Natural Environment Sciences, Faculty of Integrated Human Studies, †Department of Fundamental Energy Science, Graduate School of Energy Sciences, §Graduate School of Human and Environmental Studies, Kyoto University, Kyoto 606, Japan; ‡X-ray Research Laboratory, Rigaku Corporation, Akishima, Tokyo 196, Japan

Received November 13, 1997; in revised form May 8, 1998; accepted May 13, 1998

Ba analogues of hewettite ($CaV_6O_{16} \cdot 9H_2O$) were synthesized by the hydrothermal methods. The compounds exhibit two phases formulated by $BaV_6O_{16} \cdot nH_2O$ and $Ba_{1+x}V_6O_{16} \cdot nH_2O$ ($x \approx 0.2$, $n \approx 3$), and the structure of $BaV_6O_{16} \cdot nH_2O$ has been determined from a single crystal study. It crystallizes in the orthorhombic system *Pnmm* with $a = 12.162(3)$ Å, $b = 10.841(4)$ Å, $c = 17.035(4)$ Å, and $Z = 6$ and the structure refinements led to $R = 0.066$ and $R_w = 0.076$ for 1480 reflections with $I > 3\sigma(I)$. The structure is basically analogous to that of γ-$Li_{1+x}V_3O_8$ or $CaV_6O_{16} \cdot 9H_2O$, consisting of V_6O_{16} layers and interstitial hydrated Ba atoms. The V_6O_{16} layers stack along the *c* axis with 8.518-Å spacing which is half of the *c* axis; adjacent layers are mirror images of each other. Ba atoms reside in three kinds of sites with totally different oxygen coordinations. Their interlayer distributions result in another long period along the *b* axis which is triple the ordinary 3.6-Å period of the hewettite compounds. This is the first single-crystal structural study of the synthetic hewettite compounds.

INTRODUCTION

The hewettite family formulated by $M_2V_6O_{16} \cdot nH_2O$ for monovalent M or $MV_6O_{16} \cdot nH_2O$ for divalent M constitutes a major group in vanadium oxide minerals (1). Hewettite and metahewettite were first named in 1914 to $CaV_6O_{16} \cdot 9H_2O$ and $CaV_6O_{16} \cdot 3H_2O$, respectively (2). Subsequent extensive studies were carried out in the late 1950s and early 1960s (3–10) and discovered new members such as barnesite ($Na_2V_6O_{16} \cdot 3H_2O$) (9), hendersonite ($Ca_{1.3}V_6O_{16} \cdot 6H_2O$) (8) and grantsite ($Na_2Ca_{0.4}V_6O_{16} \cdot 4H_2O$) (10). In the same period Wadsley (11) determined the structure of γ-$Li_{1+x}V_3O_8$ which turned out to have close analogy to the structures of hewettite compounds (7). Recently γ-$Li_{1+x}V_3O_8$ has attracted much attention for its potential use in the cathode material of lithium batteries (12, 13). However, structural analyses of hewettite compounds met with extreme difficulties due to poor qualities of naturally occurred crystals. Bachmann and Barnes (7) performed the first structural study on a sodium–calcium variety ($NaCa_{0.5}V_6O_{16} \cdot 2H_2O$) in both hydrated and anhydrous forms by using visual estimates of reflections from precession and oscillation photographs. Although the results were unsatisfactory, the structural analogy to γ-$Li_{1+x}V_3O_8$ was clearly demonstrated. Recently more precise work has been made on natural hewettite ($CaV_6O_{16} \cdot 9H_2O$) by Evans (14) using precession photographs and a microdesitometer; the crystallographic data seem to be improved but still include unacceptable V-O distances of less than 1.5 Å. Their intensive efforts to clarify the structures of hewettite compounds from poor X-ray data must be highly appreciated, but more reliable structural information is desired. In the course of our hydrothermal synthesis of hewettite compounds, where the phases for M = K, Rb, Cs, NH_4, Ca, Sr, Ba were preliminarily reported (15), we successfully obtained single crystals of the Ba compound having an adequate quality for structural analysis. The present paper describes the first full structural analysis on the hewettite compound.

[1]Corresponding author. E-mail: oka@kagaku.h.kyoto-u.ac.jp.

EXPERIMENTAL

Sample Preparation

Hydrothermal synthesis of the hewettite compounds has been briefly reported (15). Here we focus on the synthesis of Ba compounds. Ba sources were 0.1–0.2 mol L^{-1} solutions of either $Ba(NO_3)_2$ or $BaCl_2$ and V sources were 300–500 mg powders of either V_2O_5 or $VO(OH)_2$. Suspensions of 80 ml Ba and V sources were sealed in Pyrex ampoules and treated in an autoclave at 250–280°C for 24–48 h. Orange-red fibrous products were separated by filtration, where BaV_2O_6 crystals (17) sometimes coexisted but were easily removed. Crystalline phases were examined by powder X-ray diffraction and compositions were determined by energy-dispersive X-ray analysis (EDX) for Ba/V atomic

0022-4596/98 $25.00

ratios, visible-light absorption for V valences, atomic absorption spectroscopy for Ba contents, and thermogravimetry (TG) for water contents. As a results, two quite similar compounds were obtained: one from V_2O_5 and one from $VO(OH)_2$, regardless of the Ba sources. The two compounds are formulated in common by $Ba_yV_6O_{16} \cdot nH_2O$ ($n \approx 3.0$), one with $y \approx 1.0$ for the V_2O_5 source and the other with $y \approx 1.2$ for the $VO(OH)_2$ source. They are well distinguished by layer spacings, namely 8.53 Å for $y \approx 1.0$ and 8.19 Å for $y \approx 1.2$. Hereafter formula of the two compounds are given by $BaV_6O_{16} \cdot nH_2O$ for $y \approx 1.0$ and $Ba_{1+x}V_6O_{16} \cdot nH_2O$ for $y \approx 1.2$. Single crystals of $BaV_6O_{16} \cdot nH_2O$ with a flat needle shape were obtained in the hydrothermal product from a $BaCl_2$-V_2O_5 suspension treated at 330°C for 55 h. The y value of the crystal was 1.00(3) and a water content of the bulk was $n = 2.7(1)$. An attempt to obtain single crystals of $Ba_{1+x}V_6O_{16} \cdot nH_2O$ was unsuccessful.

Single-Crystal X-ray Diffraction and Structure Determination

Weissenberg photographs of most crystals showed more or less elongated spots and a candidate for the structural study was selected with effort. A crystal with dimensions of $0.30 \times 0.03 \times 0.01$ mm was mounted on a Rigaku AFC7R diffractometer with monochromatized Mo$K\alpha$ radiation. The orthorhombic system was confirmed: *Pnmm* (No. 59) or $Pn2_1m$ (No. 31) with $a = 12.162(3)$ Å, $b = 10.841(4)$ Å, $c = 17.035(4)$ Å, and $Z = 6$. Data collection was made by the 2θ–ω scanning method with a scan width $\Delta\omega = (1.73 + 0.30\tan\theta)^\circ$ up to $2\theta = 80^\circ$, in which three standard reflections monitored every 150 data showed no significant intensity fluctuation. A total of 5268 reflections with $I > 0$ were obtained from which 1480 reflections with $I > 3\sigma(I)$ were used in the structure refinements. An empirical absorption correction of the ψ-scan method was applied resulting in the transmission factors of 0.844–1.000. All the data processing and the structure refinements were performed by using the TEXSAN crystallographic software package (18). The crystallographic and experimental data are listed in Table 1.

A structure model of $BaV_6O_{16} \cdot nH_2O$ was constructed by referring to the structures of γ-$Li_{1+x}V_3O_8$ (11) and $CaV_6O_{16} \cdot 9H_2O$ (14). As compared with the reference compounds $BaV_6O_{16} \cdot nH_2O$ adopts orthorhombic symmetry instead of monoclinic one and a superstructure of $b = 3 \times b_0$ and $c = 2 \times LS$, where b_0 (≈ 3.6 Å) denotes the basic b axis of the reference structures and LS denotes layer spacing. Stacking of V_6O_{16} layers of the reference compounds was modified to meet the above conditions. The V_6O_{16} layer was thus successfully derived for *Pnmm*; we adopted *Pnmm* because the statistical treatment of intensity data strongly favored centrosymmetry. Ba atoms were subsequently located in three sites of Ba(1), Ba(2), and Ba(3) in difference Fourier maps. Oxygens of interlayer water molecules were similarly located as denoted by $O_w(1)$, $O_w(2)$, $O_w(3)$, and $O_w(4)$. Metal site were confirmed to have full occupancies except for Ba(3) site whose occupancy was refined to 0.462(4). $O_w(3)$ and $O_w(4)$ sites were found to be nearly half

TABLE 1
Crystallographic Data and Experimental Parameters for $BaV_6O_{16} \cdot nH_2O$

Space group	*Pnmm*
a (Å)	12.162(3)
b (Å)	10.841(4)
c (Å)	17.035(3)
V (Å^3)	2246(2)
Z	6
D_c (gcm^{-3})	3.223
μ (cm^{-1})	62.7
No. unique reflection ($I > 0$)	5268
No. reflection ($I > 3\sigma(I)$)	1480
No. variables	128
R	0.066
R_w	0.076

TABLE 2
Atomic Parameters, Isotropic Temperature Factors and Occupancies for $BaV_6O_{16} \cdot nH_2O$

Atom	Position	x	y	z	B_{eq} (Å^2)	Occupancy
Ba(1)	2*a*	0.2541(2)	0.25	0.25	1.63(4)	1
Ba(2)	2*b*	0.9199(2)	0.75	0.25	1.15(4)	1
Ba(3)	4*e*	0.6847(2)	0.0893(4)	0.25	1.64(6)	0.462(4)
V(1)	8*g*	0.4523(2)	0.0844(3)	0.4263(1)	0.72(5)	1
V(2)	8*g*	0.7043(2)	0.0840(4)	0.4692(2)	1.11(6)	1
V(3)	8*g*	0.9327(2)	0.0862(3)	0.5518(2)	0.79(4)	1
V(4)	4*f*	0.5477(3)	0.25	0.5758(2)	0.69(8)	1
V(5)	4*f*	0.2966(4)	0.25	0.5347(3)	0.97(10)	1
V(6)	4*f*	0.0683(4)	0.25	0.4383(3)	0.70(8)	1
O(1)	8*g*	0.3786(9)	0.092(1)	0.3480(6)	1.3(2)	1
O(2)	8*g*	0.9822(8)	0.099(1)	0.6381(6)	1.4(2)	1
O(3)	8*g*	0.5541(8)	0.080(1)	0.5448(6)	0.7(2)	1
O(4)	8*g*	0.5885(8)	0.0867(10)	0.3900(5)	0.8(2)	1
O(5)	8*g*	0.6769(9)	−0.0836(10)	0.4887(6)	0.9(2)	1
O(6)	8*g*	0.8028(9)	0.085(1)	0.4072(6)	1.5(2)	1
O(7)	8*g*	0.7909(7)	0.085(1)	0.5647(6)	0.7(2)	1
O(8)	8*g*	0.0507(8)	0.082(1)	0.4712(6)	1.1(2)	1
O(9)	4*f*	0.618(1)	0.25	0.653(1)	1.5(3)	1
O(10)	4*f*	0.033(1)	0.25	0.345(1)	2.2(4)	1
O(11)	4*f*	0.448(1)	0.25	0.4612(10)	0.7(3)	1
O(12)	4*f*	0.411(1)	0.25	0.6117(9)	1.1(3)	1
O(13)	4*f*	0.672(2)	0.25	0.491(1)	1.0(3)	1
O(14)	4*f*	0.196(1)	0.25	0.596(1)	1.4(3)	1
O(15)	4*f*	0.211(1)	0.25	0.436(1)	1.6(4)	1
O(16)	4*f*	0.943(1)	0.25	0.5109(8)	0.3(2)	1
$O_w(1)$	2*b*	0.181(2)	0.75	0.25	2.7(5)	1
$O_w(2)$	4*e*	0.164(2)	0.022(2)	0.25	4.7(5)	1
$O_w(3)$	4*e*	0.535(2)	0.940(3)	0.25	2.7(6)	0.5
$O_w(4)$	4*e*	0.698(3)	0.670(3)	0.25	2.5(7)	0.5

occupied and therefore their occupancies were fixed at 0.5. Their half occupancies will be discussed later on the structural basis. All the oxygen atoms were refined isotropically because a few oxygens showed almost zero or even negative values for the diagonal components of anisotropic displacement factors (U_{ii}) presumably due to poor quality and highly anisotropic shape of the crystal. We encountered the same problem in the previous study on other hydrated layered vanadium oxides δ-$M_{0.25}V_2O_5 \cdot H_2O$ (M = Ca, Ni) (19). The refinements finally converged on $R = 0.066$ and $R_w = 0.076$. Atomic parameters and temperature factors are listed in Table 2.

The composition determined by the X-ray study is $Ba_{0.975(3)}V_6O_{16} \cdot 1.67H_2O$ in good agreement with $Ba_{1.00(3)}V_6O_{16} \cdot 2.7(1)H_2O$ by the chemical analysis especially in the Ba content. However, the water content by the X-ray study is somewhat lower than that by the chemical analysis, indicating that all the water molecules could not be located. This may be due to that some of water molecules do not reside in crystallographic sites or in other words disperse around Ba atoms. Actually in our previous study on other barium vanadium oxide $Ba_{0.4}V_3O_8(VO)_{0.4} \cdot nH_2O$ (20) water molecules coordinated to interstitial Ba atoms was failed to be fully located: $n = 0.41$ by the X-ray study while $n \approx 0.6$ by the chemical analysis.

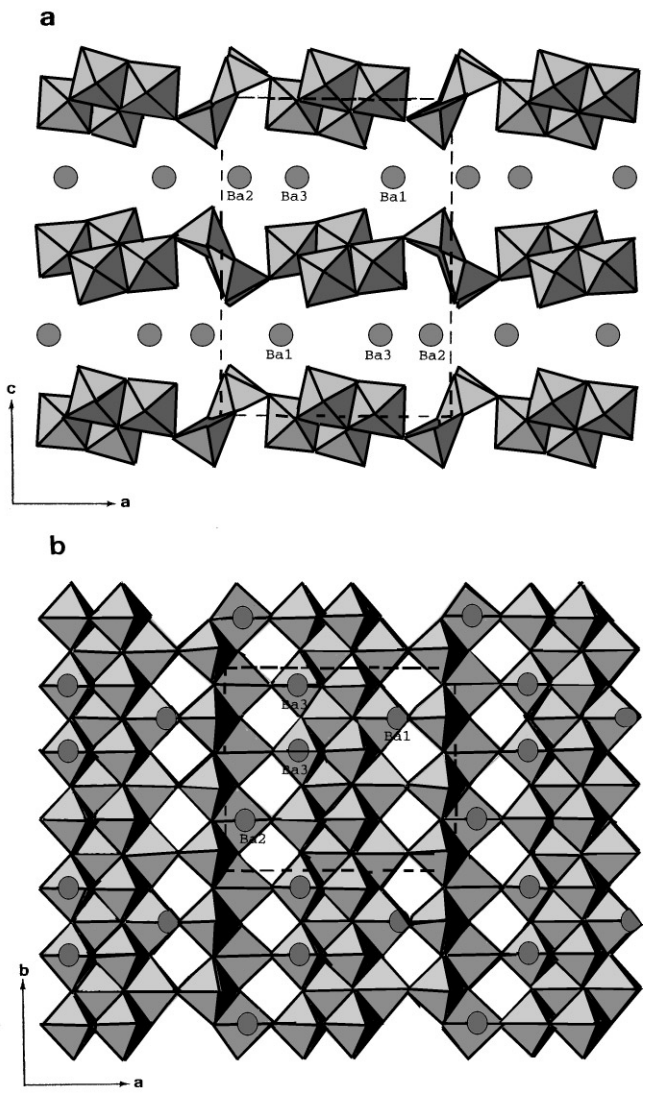

FIG. 1. Crystal structure of $BaV_6O_{16} \cdot nH_2O$ viewed along (a) the b axis and (b) the c axis. V_6O_{16} layers are drawn by polyhedral representation and Ba atoms are denoted by circles. Dashed lines represent the unit cell.

RESULTS AND DISCUSSION

Structure of V_6O_{16} Layers

Figure 1 depicts the overall structure of $BaV_6O_{16} \cdot nH_2O$ consisting of V_6O_{16} layers and interlayer Ba atoms. The V_6O_{16} layer is structurally similar to that of γ-$Li_{1+x}V_3O_8$ or $CaV_6O_{16} \cdot 9H_2O$, indicating that $BaV_6O_{16} \cdot nH_2O$ is certainly a member of the hewettite group. As depicted in Fig. 2, the V_6O_{16} framework is built up with VO_6 octahedra of V(1), V(2), V(4) and V(5), and VO_5 trigonal bipyramids of V(3) and V(6), for which V–O bond distances and O–V–O bond angles are listed in Table 3. VO_6 octahedra are joined by sharing edges to form a double chain running along the b axis and similarly edge-sharing VO_5 trigonal bipyramids form a single chain (Fig. 1b). Both ribbons are connected through O(7) and O(15) vertices along the a axis forming the V_6O_{16} framework. All the V–O polyhedra, especially VO_6 octahedra, are highly distorted as usually found in V(V, IV) oxides. As seen in Fig. 1a, the c period is twice the layer stacking sequence, where adjacent V_6O_{16} layers are placed to form mirror images of each other. A similar double-period structure is found in the stacking mode of V_2O_5 layers of the *orthorhombic* $K_{0.5}V_2O_5$ (20, 21) while it is not adopted by the *monoclinic* $K_{0.5}V_2O_5$ (22). The V_6O_{16} structure has been described and discussed in the previous papers (7, 11, 13, 14) and thus no further description is given here.

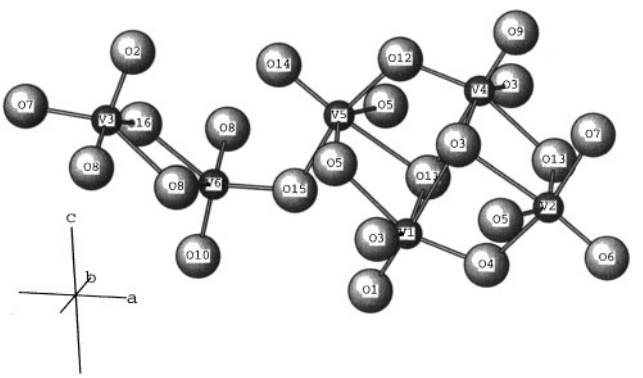

FIG. 2. V–O framework of the V_6O_{16} layer. V and O atoms are denoted by small and large circles, respectively.

TABLE 3
Bond Distances (Å) Angles (°) for V–O Polyhedra

$V(1)O_6$ octahedron								
V(1)–O(1)	1.61(1)	V(1)–O(3)	2.37(1)	V(1)–O(3)[a]	1.85(2)			
V(1)–O(4)	1.77(1)	V(1)–O(5)[a]	2.14(1)	V(1)–O(11)	1.892(8)			
O(1)–V(1)–O(3)	177.0(8)	O(1)–V(1)–O(3)[a]	104.3(9)					
O(1)–V(1)–O(4)	103.4(7)	O(1)–V(1)–O(5)[a]	98.8(8)					
O(1)–V(1)–O(11)	101.3(9)	O(3)–V(1)–O(3)[a]	77.0(8)					
O(3)–V(1)–O(4)	79.0(6)	O(3)–V(1)–O(5)[a]	78.9(7)					
O(3)–V(1)–O(11)	76.5(9)	O(3)[a]–V(1)–O(4)	98.4(8)					
O(3)[a]–V(1)–O(5)[a]	77.6(7)	O(3)[a]–V(1)–O(11)	146.0(9)					
O(4)–V(1)–O(5)[a]	157.8(6)	O(4)–V(1)–O(11)	97.0(9)					
O(5)[a]–V(1)–O(11)	76.7(9)							
$V(2)O_6$ octahedron								
V(2)–O(3)	2.24(1)	V(2)–O(4)	1.95(1)	V(2)–O(5)	1.88(1)			
V(2)–O(6)	1.60(2)	V(2)–O(7)	1.94(1)	V(2)–O(13)	1.877(9)			
O(3)–V(2)–O(4)	79.0(6)	O(3)–V(2)–O(5)	74.6(8)					
O(3)–V(2)–O(6)	173.7(8)	O(3)–V(2)–O(7)	87.7(6)					
O(3)–V(2)–O(13)	87.7(9)	O(4)–V(2)–O(5)	90.5(7)					
O(4)–V(2)–O(6)	94.8(8)	O(4)–V(2)–O(7)	166.6(7)					
O(4)–V(2)–O(13)	88.4(9)	O(5)–V(2)–O(6)	104.9(9)					
O(5)–V(2)–O(7)	87.3(8)	O(5)–V(2)–O(13)	148.8(8)					
O(6)–V(2)–O(7)	98.5(7)	O(6)–V(2)–O(13)	106.3(9)					
O(7)–V(2)–O(13)	86.7(9)							
$V(3)O_5$ trigonal bipyramid								
V(3)–O(2)	1.60(1)	V(3)–O(7)	1.74(1)	V(3)–O(8)[b]	1.99(1)			
V(3)–O(8)[a]	1.88(2)	V(3)–O(16)	1.911(8)					
O(2)–V(3)–O(7)	105.0(7)	O(2)–V(3)–O(8)[b]	111.5(7)					
O(2)–V(3)–O(8)[a]	103.7(8)	O(2)–V(3)–O(16)	103.3(8)					
O(7)–V(3)–O(8)*b*	143.5(7)	O(3)–V(3)–O(8)[a]	97.2(8)					
O(3)–V(3)–O(16)	96.8(8)	O(8)[b]–V(3)–O(8)[a]	75.988)					
O(8)[b]–V(3)–O(16)	73.9(8)	O(8)[a]–V(3)–O(16)	145.1(7)					
$V(4)O_6$ octahedron								
V(4)–O(3)	1.92(2)	V(4)–O(3)[c]	1.92(2)	V(4)–O(9)	1.57(2)			
V(4)–O(11)	2.30(2)	V(4)–O(12)	1.77(2)	V(4)–O(13)	2.10(2)			
O(3)–V(4)–O(3)[c]	147.7(9)	O(3)–V(4)–O(9)	102.0(6)					
O(3)–V(4)–O(11)	77.7(6)	O(3)–V(4)–O(12)	97.6(6)					
O(3)–V(4)–O(13)	77.3(6)	O(3)[c]–V(4)–O(9)	102.0(6)					
O(3)[c]–V(4)–O(11)	77.7(6)	O(3)[c]–V(4)–O(12)	97.6(6)					
O(3)[c]–V(4)–O(13)	77.3(7)	O(9)–V(4)–O(11)	178.8(9)					
O(9)–V(4)–O(12)	102.8(9)	O(9)–V(4)–O(13)	100.7(9)					
O(11)–V(4)–O(12)	78.4(9)	O(11)–V(4)–O(13)	78.1(9)					
O(12)–V(4)–O(13)	156.5(9)							
$V(5)O_6$ octahedron								
V(5)–O(5)[a]	1.88(1)	V(5)–O(5)[d]	1.88(1)	V(5)–O(11)	2.22(2)			
V(5)–O(12)	1.92(1)	V(5)–O(14)	1.60(3)	V(5)–O(15)	1.98(3)			
O(5)[a]–V(5)–O(5)[d]	148.3(9)	O(5)[a]–V(5)–O(11)	74.8(6)					
O(5)[a]–V(5)–O(12)	91.2(6)	O(5)[a]–V(5)–O(14)	105.6(6)					
O(5)[a]–V(5)–O(15)	84.8(6)	O(5)[d]–V(5)–O(11)	74.8(6)					
O(5)[d]–V(5)–O(12)	91.2(6)	O(5)[d]–V(5)–O(14)	105.6(6)					
O(5)[d]–V(5)–O(15)	84.8(7)	O(11)–V(5)–O(12)	77.5(9)					
O(11)–V(5)–O(14)	173.7(9)	O(11)–V(5)–O(15)	87.5(9)					
O(12)–V(5)–O(14)	96.2(9)	O(12)–V(5)–O(15)	165.1(9)					
O(14)–V(5)–O(15)	98.7(9)							
$V(6)O_5$ trigonal bipyramid								
V(6)–O(8)	1.92(2)	V(6)–O(8)[c]	1.92(2)	V(6)–O(10)	1.64(3)			
V(6)–O(15)	1.73(2)	V(6)–O(16)[e]	1.96(2)					
O(8)–V(6)–O(8)[c]	143.5(9)	O(8)–V(6)–O(10)	104.7(6)					
O(8)–V(6)–O(15)	96.8(6)	O(8)–V(6)–O(16)[c]	74.3(5)					
O(8)[c]–V(6)–O(10)	104.7(6)	O(8)[c]–V(6)–O(15)	96.8(6)					
O(8)[c]–V(6)–O(16)[e]	74.3(5)	O(10)–V(6)–O(15)	103.8(9)					
O(10)–V(6)–O(16)[e]	113.9(9)	O(15)–V(6)–O(16)[e]	142.2(9)					

Symmetry code: [a] $1-x,-y,1-z$; [b] $x,y,z+1$; [c] $x,1/2-y,z$; [d] $1-x,y+1/2,1-z$; [e] $x,y,z-1$.

Interlayer Ba Distributions

Interlayer Ba atoms reside in three kinds of sites Ba(1), Ba(2), and Ba(3) on the mirror plane ($z = 0.25, 0.75$) between V_6O_{16} layers. As seen in Fig. 1b, the Ba distributions are responsible for the $3 \times b_0$ period along the b axis. Ba–O (including $-O_w$) distances are listed in Table 4 and Ba–O coordinations are depicted in Fig. 3. Ba(1) and Ba(2) sites are fully occupied while Ba(3) site is half occupied; adjacent Ba(3) sites are unlikely to be occupied simultaneously since the Ba(3)–Ba(3) distance of 3.48(1) Å is fairly short judging from that Ba–Ba distances are usually above 3.6 Å in barium oxide compounds. With full occupancies of Ba(1) and Ba(2) sites and half occupancy of Ba(3) site, BaV_6O_{16} becomes a stoichiometric formula. As depicted in Fig. 3, Ba atoms exhibit different Ba–O coordinations with oxygens of V_6O_{16} layers, forming polyhedra of $Ba(1)O_8$, $Ba(2)O_6$, and $Ba(3)O_4$. $Ba(1)O_8$ is a bicapped trigonal prism, $Ba(2)O_6$ a distorted trigonal prism, and $Ba(3)O_4$ a coplaner rectangle. Bond valence sums (BVS) (24) of Ba for these Ba–O polyhedra become similar values of 1.34 for Ba(1), 1.38 for Ba(2), and 1.00 for Ba(3). Deficient bond valences of 0.62–1.00 must be provided by interlayer water (O_w). There are four O_w sites located by the X-ray study; $O_w(1)$ and $O_w(2)$ are fully occupied, while $O_w(3)$ and $O_w(4)$ are half occupied. Their distributions around Ba atoms are illustrated in Fig. 4. Both $O_w(3)$ and $O_w(4)$ must have half occupancy because $O_w(3)$ coordinates to half occupied Ba(3) and because simultaneous occupation in neighboring $O_w(4)$ sites is prevented due to the short $O_w(4)$–$O_w(4)$ distance of 1.81(1) Å. Ba(1) is coordinated by two $O_w(2)$ which cap two

TABLE 4
Ba–O Distances (Å) for Ba–O Polyhedra

Ba(1)–O			
Ba(1)–O(1)[a,b,c,d]	2.83(1)	Ba(1)–O(10)[a,b]	3.14(2)
Ba(1)–O(15)[a,b]	3.21(3)	Ba(1)–O_w(2)[a,c]	2.70(3)
Ba(2)–O			
Ba(2)–O(2)[e,f,g,h]	2.78(1)	Ba(2)–O(14)[i,j]	2.98(3)
Ba(2)–O_w(1)[k]	3.18(4)	Ba(1)–O_w(4)[a,l]	2.83(5)
Ba(3)–O			
Ba(3)–O(4)[a,b]	2.66(1)	Ba(3)–O(6)[a,b]	3.04(2)
Ba(3)–O_w(3)[m]	2.43(4)	Ba(1)–O_w(4)[c]	2.81(5)

Symmetry codes: [a] x,y,z; [b] $x,y,1/2-z$; [c] $x,1/2-y,z$; [d] $x,1/2-y,1/2-z$; [e] $2-x,1/2+y,z-1/2$; [f] $2-x,1-y,z-1/2$; [g] $2-x,1/2+y,1-z$; [h] $2-x,1-y,1-z$; [i] $1-x,1-y,z-1/2$; [j] $1-x,1-y,1-z$; [k] $1+x,y,z$; [l] $x,3/2-y,z$; [m] $x,y-1,z$.

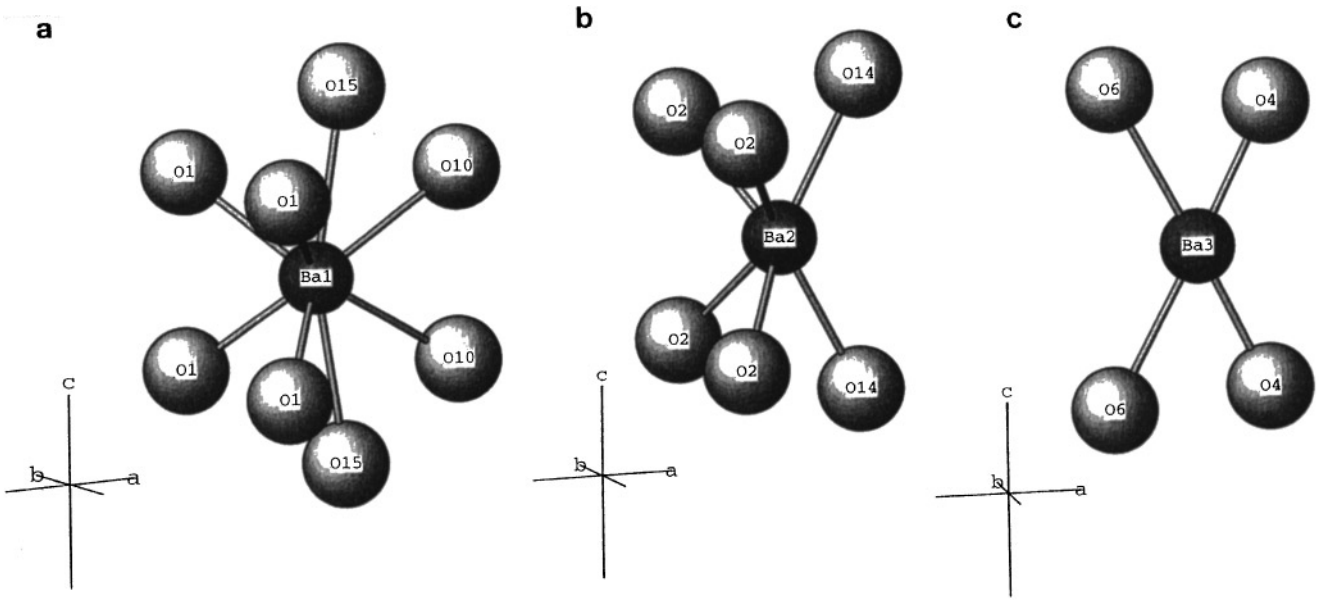

FIG. 3. Ba–O coordinations for (a) $Ba(1)O_8$, (b) $Ba(2)O_6$, and (c) $Ba(3)O_4$.

side walls of the $Ba(1)O_8$, leading to a tricapped $Ba(1)O_{10}$ trigonal prism. Then the BVS of Ba(1) becomes a proper value of 1.99. Ba(2) is coordinated by one $O_w(1)$ and one of two $O_w(4)$ forming a $Ba(2)O_8$ polyhedra and its BVS becomes 1.71. Ba(3) appears to be coordinated by one $O_w(3)$ and one $O_w(4)$ but the $O_w(3)$–$O_w(4)$ distance of 2.31(1) Å is too short to place $O_w(4)$ next to $O_w(3)$. Consequently Ba(3) is coordinated by one $O_w(3)$ with a fairly short distance of 2.43(4) Å, yielding a BVS of 1.67. Therefore excess water molecules, which failed to be located, should exist around Ba(2) and Ba(3).

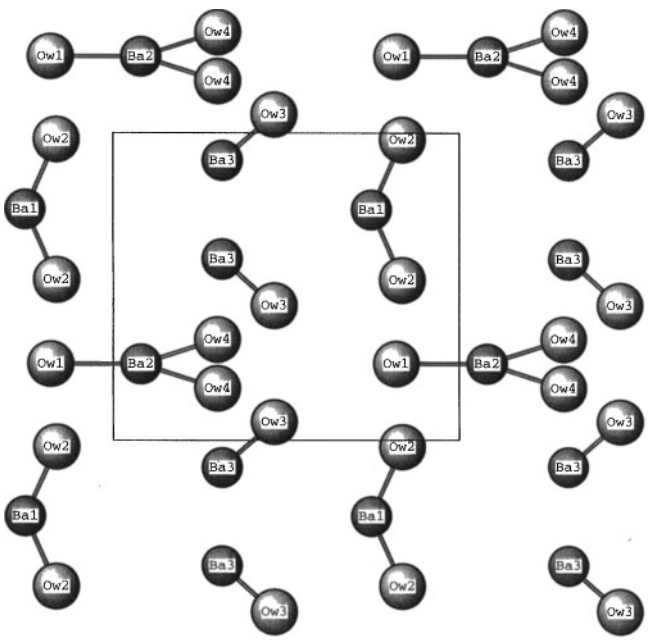

FIG. 4. Coordination of interlayer water (O_w) to Ba atoms in the *ab* plane. Solid lines represent the *ab* plane unit.

Hewettite Phases Related to $BaV_6O_{16}\cdot nH_2O$

A series of hewettite compounds are hydrothermally synthesized by incorporating alkali metals and alkaline-earth metals as interlayer material (15). Unit cell parameters for the hydrothermally-synthesized compounds are listed in Table 5, together with selected literature data. The hydrothermal alkali metal compounds are generally formulated $M_2V_6O_{16}\cdot nH_2O$ ($n \approx 3$) for M = K, Rb, Cs, NH_4, and crystallize in *P*-type monoclinic systems. Their *c* axes correspond to doubled layer spacings ($2\times LS$), which is sometimes observed in the hewettite compounds (Table 5). The structural details of the alkali metal compounds remain unknown.

The hydrothermal alkaline–earth metal compounds are formed for M = Ca, Sr, Ba (Table 5), of which the Ca compound is undoubtedly identical to the natural hewettite $CaV_6O_{16}\cdot 9H_2O$ and the Sr and Ba compounds are new members as well as the alkali metal compounds. All the phases of the Sr and Ba compounds adopt *P*-type orthorhombic systems with $c = 2\times LS$.

The Ba compounds are further divided into two phases designated by $BaV_6O_{16}\cdot nH_2O$ and $Ba_{1+x}V_6O_{16}\cdot nH_2O$, as mentioned before. $Ba_{1+x}V_6O_{16}\cdot nH_2O$ is regarded as a reduced form of $BaV_6O_{16}\cdot nH_2O$, exhibiting a shorter layer

TABLE 5
Crystallographic Data for Synthetic Akali–Metal and Alkali–Earth–Metal Compounds, Hewettite-Group Minerals and γ-Lithium Vanadium Bronzes

Compound	a/Å	b/Å	c/Å	b/°	LS[a]/Å	Ref.
Alkali-metal compounds ($n \approx 1.5$)						
$K_2V_6O_{16}\cdot nH_2O$	12.296(7)	3.5987(8)	16.015(2)	93.89(3)	7.989	(15)
$Rb_2V_6O_{16}\cdot nH_2O$	12.313(2)	3.5800(7)	16.456(2)	94.58(2)	8.202	(15)
$Cs_2V_6O_{16}\cdot nH_2O$	12.272(7)	3.5948(8)	17.087(5)	99.35(5)	8.430	(15)
$(NH_4)_2V_6O_{16}\cdot nH_2O$	12.343(6)	3.5922(7)	16.410(6)	93.30(4)	8.191	(15)
Alkali-earth-metal compounds						
$CaV_6O_{16}\cdot nH_2O$ ($n \approx 9$)	12.308(8)	3.5982(8)	11.234(6)	97.17(3)	11.146	(15)
$SrV_6O_{16}\cdot nH_2O$ ($n \approx 3$)	12.120(8)	3.6102(5)	16.448(4)	90	8.224	(15)
$BaV_6O_{16}\cdot nH_2O$ ($n \approx 3$)	12.158(5)	10.838(2)	17.057(6)	90	8.529	This work
$Ba_{1.2}V_6O_{16}\cdot nH_2O$ ($n \approx 3$)	12.253(4)	3.5993(5)	16.384(4)	90	8.192	This work
Hewettite group minerals						
hewettite $CaV_6O_{16}\cdot 9H_2O$	12.290(1)	3.590(1)	11.174(2)	97.24(1)	11.085	(14)
metahewettite $CaV_6O_{16}\cdot 3H_2O$	12.15(1)	3.607(3)	18.44(1)	118.03(3)	8.14	(16)
barnesite $Na_2V_6O_{16}\cdot 3H_2O$	12.17(4)	3.602(10)	7.78(4)	95.0(4)	7.75	(9)
hendarsonite $Ca_{1.3}V_6O_{16}\cdot 6H_2O$	12.40(4)	10.77(3)	18.92(8)	90	9.46	(8)
grantsite $Na_2Ca_{0.4}V_6O_{16}\cdot 4H_2O$	12.41(4)	3.60(1)	17.54(6)	95.3(2)	8.73	(10)
γ-Lithium vanadium bronze						
$Li_{1+x}V_3O_8$	12.03(2)	3.60(1)	6.68(2)	107.8	6.36	(11)
$Li_{1.2}V_3O_8$	11.862	3.559	6.596	107.66	6.285	(13)
$Li_4V_3O_8$	11.915	3.911	5.955	107.03	5.686	(13)

[a] *LS* denotes layer spacing.

spacing and a higher Ba content with respect to $BaV_6O_{16}\cdot nH_2O$. The phase formation in the hydrothermal synthesis depends on the starting vanadium sources; V_2O_5 of V(V) yields $BaV_6O_{16}\cdot nH_2O$ while $VO(OH)_2$ of V(IV) yields $Ba_{1+x}V_6O_{16}\cdot nH_2O$. In the case of $VO(OH)_2$ most of V(IV) species are oxidized to V(V) under hydrothermal conditions, forming $Ba_{1+x}V_6O_{16}\cdot nH_2O$ with an average vanadium oxidation of 4.93 for $x = 0.2$, where further oxidation results in biphasic products with $BaV_6O_{16}\cdot nH_2O$. As demonstrated in Fig. 5 by the change in X-ray diffraction patterns, it is noted that $Ba_{1+x}V_6O_{16}\cdot nH_2O$ is converted from $BaV_6O_{16}\cdot nH_2O$ by reducing $BaV_6O_{16}\cdot nH_2O$ in a BaI_2 solution, where V reduction is accompanied by Ba insertion. $Ba_{1+x}V_6O_{16}\cdot nH_2O$ is also clearly distinguished from other hewettite members in the plot of layer spacings versus ionic radii of interlayer cations as shown in Fig. 6. The layer spacings of the hewettite members having similar degrees of hydration both for alkali metals and alkaline–earth metals are well proportional to the interlayer cationic radii, except for that of $Ba_{1+x}V_6O_{16}\cdot nH_2O$ which comes well below the proportional line. The exact structure of $Ba_{1+x}V_6O_{16}\cdot nH_2O$ has not yet been determined but it is presumed that its V_6O_{16} layer is identical to that of $BaV_6O_{16}\cdot nH_2O$ while its Ba distribution must greatly differ to reduce the $3\times b_0$ period of $BaV_6O_{16}\cdot nH_2O$.

$BaV_6O_{16}\cdot nH_2O$ exhibits the $3\times b_0$ and $2\times LS$ superstucture with orthorhombic symmetry. The present study has revealed that the $3\times b_0$ period originates from the Ba distribution and the $2\times LS$ from the stacking mode of V_6O_{16} layers. The $3\times b_0$ and $2\times LS$ periods with orthorhombic symmetry was reported in a hewettite group member of hendersonite $Ca_{1.3}V_6O_{16}\cdot 6H_2O$ (8) (Table 5) which was claimed to have space group *Pnam* (No. 62) or $Pn2_1a$ (No.

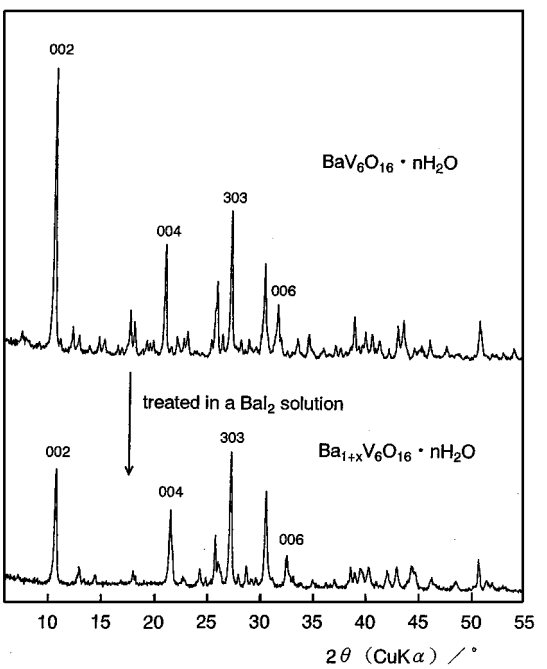

FIG. 5. Change in X-ray diffraction patterns from $BaV_6O_{16}\cdot nH_2O$ (top) to $Ba_{1+x}V_6O_{16}\cdot nH_2O$ (bottom) by treatment in a barium iodide solution.

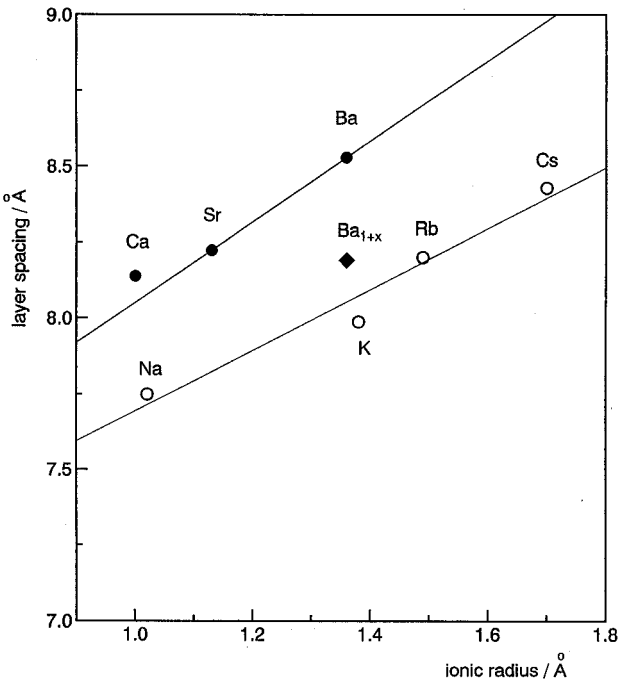

FIG. 6. Plots of layer spacing vs ionic radius of interlayer M^{n+} ion for hewettite group compounds: $MV_6O_{16}\cdot nH_2O$ ($n \approx 3$) with M^{2+} (M = Ca, Sr, Ba) and $M_2V_6O_{16}\cdot nH_2O$ ($n \approx 1.5$) with M^{+} (M = Na, K, Rb, Cs) denoted by closed and open circles, respectively. Ba_{1+x} denoted by a closed diamond represents $Ba_{1+x}V_6O_{16}\cdot nH_2O$. Data are taken from Table 5.

33), but its structure remains unknown. No other type of superstructure has been reported in the hewettite group. Recently another superstructure has been found in the δ-type layered bronze $Sr_{0.5}V_2O_5$ (25) which exhibits a $2\times a_\delta$ and $2\times b_\delta$ superstructure, where a_δ (≈ 11.7 Å) and b_δ (≈ 3.6 Å) denote the basic δ-type V_2O_5 layer lattice periods. The ordered distribution of interlayer Sr atoms results in superstructure just like that of Ba atoms in $BaV_6O_{16}\cdot nH_2O$.

ACKNOWLEDGMENT

The present work is supported by a Grant-in-Aid for Scientific Research from the Ministry of Education, Science, Sports and Culture of Japan.

REFERENCES

1. H. T. Evans Jr. and J. M. Hughes, *Amer. Miner.* **75,** 508 (1900).
2. W. F. Hillebrand, H. E. Merwin, and F. E. Wright, *Proc. Am. Phil. Soc.* **53,** 31 (1914).
3. W. H. Barnes, *Amer. Miner.* **40,** 689 (1955).
4. M. Ross, *Am. Miner.* **44,** 322 (1959).
5. A. Weiss, K, Hartl, and E. Michel, *Z. Naturforsch. B* **16,** 842 (1961).
6. M. M. Qurashi, *Can. Miner.* **6,** 647 (1961).
7. H.-G. Bachmann and W. H. Barnes, *Can. Miner.* **7,** 219 (1962).
8. M. L. Lindberg, A. D. Weeks, M. E. Thompson, D. P. Elston, and R. Meyrowitz, *Amer. Miner.* **47,** 1252 (1962).
9. A. D. Weeks, D. R. Ross, and R. F. Marvin, *Am. Miner.* **48,** 1187 (1963).
10. A. D. Weeks, M. L. Lindberg, A. H. Truesdell, and R. Meyrowitz, *Am. Miner.* **49,** 1511 (1964).
11. A. D. Wadsley, *Acta Crystallogr.* **10,** 261 (1957).
12. K. West, B. Zachau-Christiansen, S. Skaarup, Y. Saidi, J. Barker, I. I. Olsen, R. Pynenburg, and R. Koksbang, *J. Electrochem. Soc.* **143,** 820 (1996). [Ref. therein.]
13. L. A. de Picciotto, K. T. Adendroff, D. C. Liles, and M. M. Thackeray, *Solid State Ionics* **62,** 297 (1993).
14. H. T. Evans Jr., *Can. Miner.* **6,** 181 (1989).
15. Y. Oka, T. Yao, and N. Yamamoto, in *Solvo-Thermaal Reactions, Vol. 1, Proc. 1st Internat. Conf. Solvo-Thermal Reactions 1994 Takamatsu Japan,* p. 197.
16. P. Bayliss and S. S. J. Warne, *Miner. Mag.* **43,** 550 (1979).
17. T. Yao, Y. Oka, and N. Yamamoto, *Inorg. Chim. Acta* **238,** 165 (1995).
18. *TEXSAN: Crystal Structure Analysis Package*, Molecular Structure Corp., the Woodland, TX, 1985–1992.
19. Y. Oka, T. Yao, and N. Yamamoto, *J. Solid State Chem.* **132,** 323–329 (1997).
20. Y. Oka, O. Tamada, T. Yao, and N. Yamamoto, *J. Solid State Chem.* **114**, 359 (1995).
21. Y. Kanke, K. Kato, E. Takayama-Muromachi, M. Isobe, and K. Kosuda, *Acta Crystallogr. Sect. C* **46,** 1590 (1990).
22. J-M. Savariault and J. Galy, *J. Solid State Chem.* **101,** 119 (1992).
23. Y. Oka, T. Yao, and N. Yamamoto, *J. Mater. Chem.* **5,** 1423 (1995).
24. I. D. Brown and K. K. Wu, *Acta Crystallogr. Sect. B* **32,** 1957 (1976).
25. K. Kato, Y. Kanke, Y. Oka, and T. Yao, *Z. Kristallogr.*, in press.